An Effective Field Theory Analysis of the LUX WIMP Search

Nicole A. Larsen
Yale University
The LUX Collaboration

NDM ’15
Jyväskylä, Finland
3 June 2015

Xenon as a Direct Detection Target

- High density (3 g/cm^3) and high atomic mass (A = 131 g/mol)
- Scintillates brightly in the near-UV (178 nm) with fast (ns) response time
- Excellent ionization threshold and long electron drift lengths (~1 m)
- High abundance of odd isotopes => spin-dependent sensitivity.

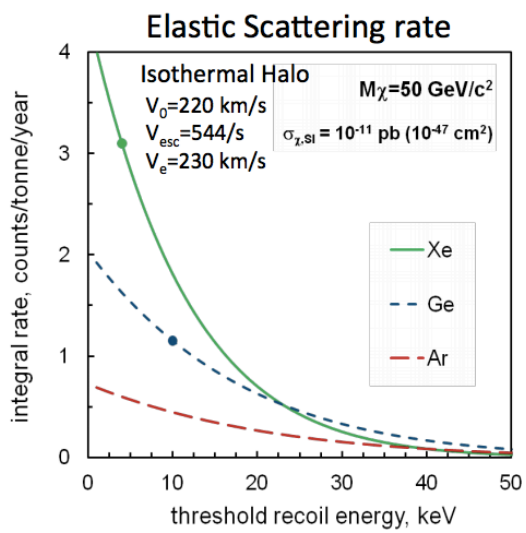

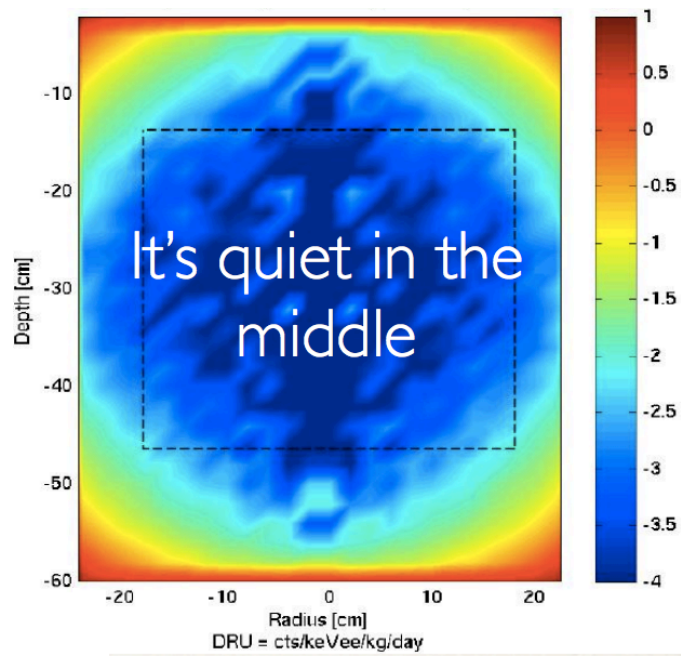

- No long-lived intrinsic backgrounds
- Scalable to multi-ton size
- Self-shielding possible with 3D reconstruction

Dual-Phase TPCs: Principle of Operation

- The target is cooled to condensation point => liquid topped by a thin layer of gas.
- An incident particle excites/ionizes a target atom, which emits primary scintillation ("S1") light.
- Ionization electrons produced are drifted upwards by an applied electric field and extracted into the gas phase, where they are accelerated rapidly and caused to scintillate again ("proportional" or "S2" light).

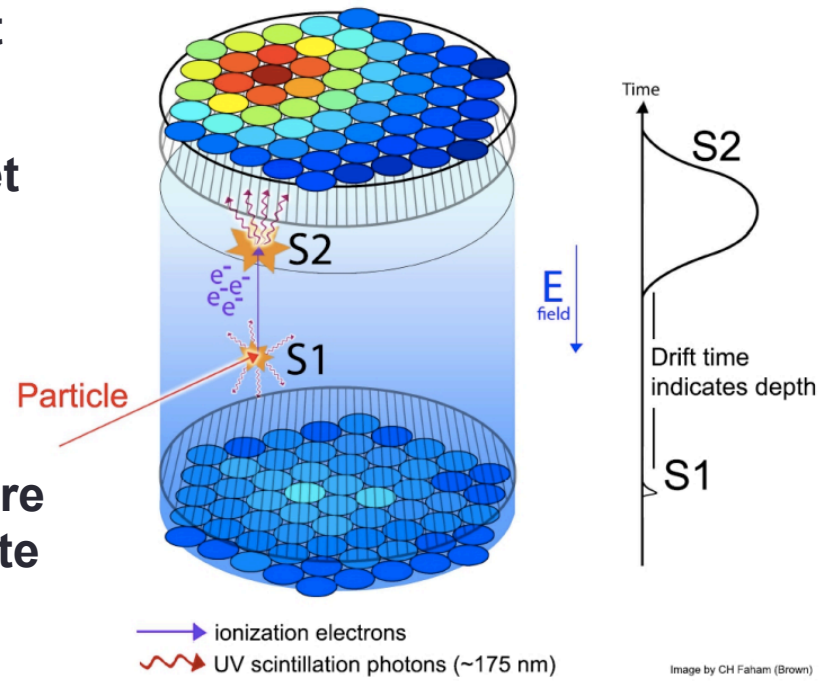

3D imaging possible:

Timing between the S1 and S2 pulses yields z-position.

PMT hit patterns yield xy-position.

ER/NR discrimination possible:

Nuclear recoils produce dense tracks

Electron recoils produce less-dense tracks

=> $(S2/S1)_{\gamma} >> (S2/S1)_{neutron}$

The Large Underground Xenon Experiment

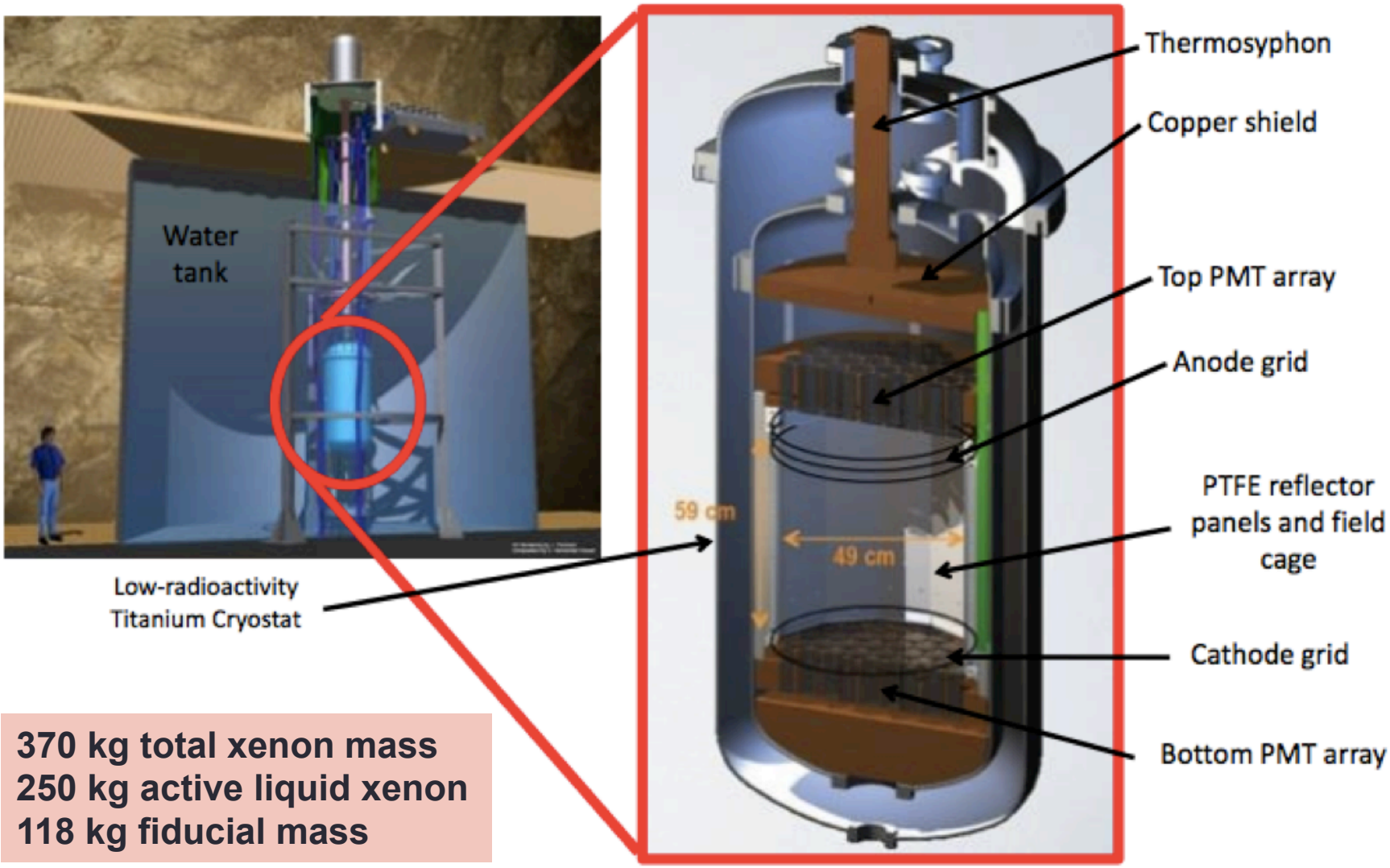

370 kg total xenon mass
250 kg active liquid xenon
118 kg fiducial mass

LUX instrument paper: NIM A 704 11-126(2013) (arXiv:1211.3788)

LUX Internals

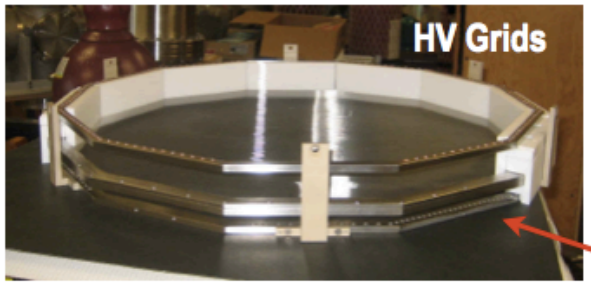

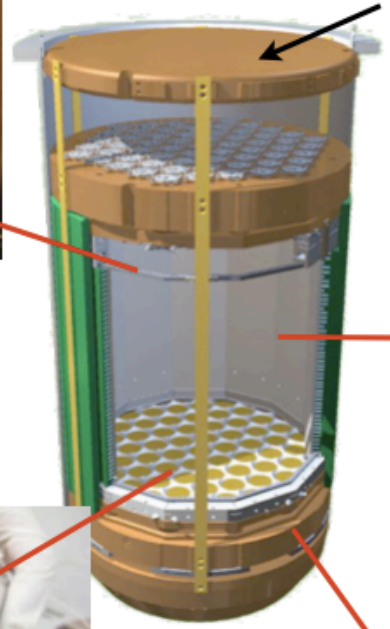

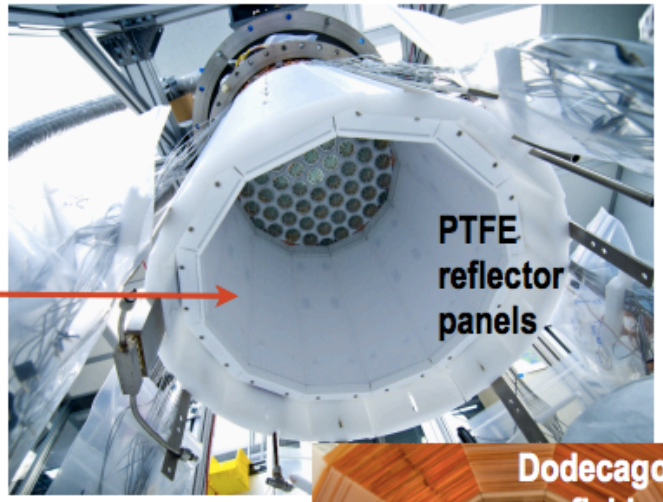

122 2" PMTs (Hamamatsu R8778)

- QE (175 nm) ~33%
- U/Th ~9/3 mBq/PMT

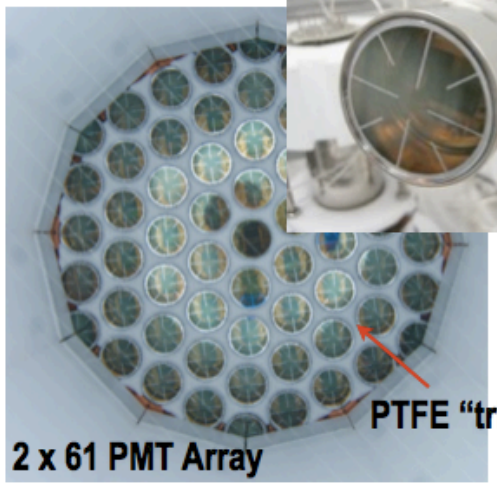

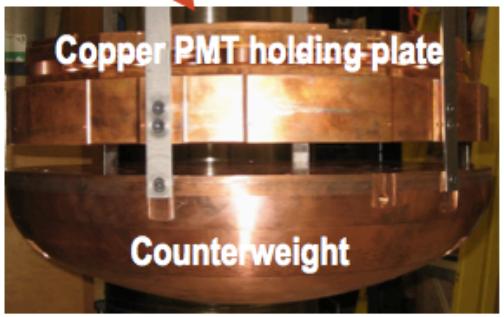

LUX First Underground Run - Highlights

- 85.3 livedays of data collected
- Xenon purity: e^- drift length 87-135 cm
  - Continuous circulation at 250 kg/day through an external purifier
  - Monitored weekly using ^{83m}Kr injections
- Drift field: 181 V/cm (speed 1.5 mm/μs) with 99.6% ER discrimination
- Light collection efficiency: 14% (includes detector geometry and PMT QE; 3D corrections provided by ^{83m}Kr calibrations)
- Fiducial mass: 118.3 +/- 6.5 kg
  - Selection based on α events from grids and teflon
- WIMP-search window: ~3-25 keVnr

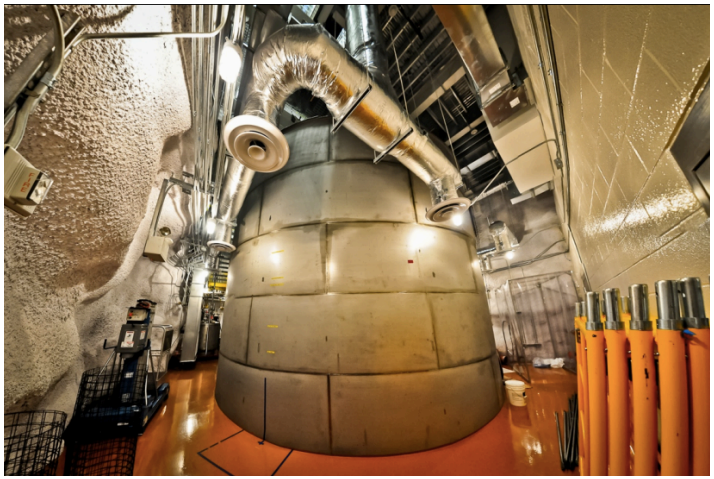

Event Selection and Cuts

Cut	Explanation	Events Remaining
All Triggers	S2 Trigger >99% for $S2_{raw}$>200 phe	83,673,413
Detector Stability	Cut periods of excursion for Xe Gas Pressure, Xe Liquid Level, Grid Voltages	82,918,901
Single Scatter Events	Identification of S1 and S2. Single Scatter cut.	6,585,686
S1 energy	Accept 2-30 phe (energy ~ 0.9-5.3 keVee, ~3-18 keVnr)	26,824
S2 energy	Accept 200-3300 phe (>8 extracted electrons) Removes single electron / small S2 edge events	20,989
S2 Single Electron Quiet Cut	Cut if >100 phe outside S1+S2 identified +/-0.5 ms around trigger (0.8% drop in livetime)	19,796
Drift Time Cut away from grids	Cutting away from cathode and gate regions, 60 < drift time < 324 us	8731
Fiducial Volume radius and drift cut	Radius < 18 cm, 38 < drift time < 305 us, 118 kg fiducial	160

Only simple, obvious cuts – no tuning beyond selecting a threshold, higher energy cutoff, and fiducial volume.

The LUX First WIMP-Search Result

- **After all selection cuts, 160 candidate events left in the fiducial volume**
- **Distribution is consistent with electron recoil background and no WIMP signal with a p-value of 0.35 from Profile-Likelihood Ratio Analysis with incorporated background models, detector effects, and efficiencies**

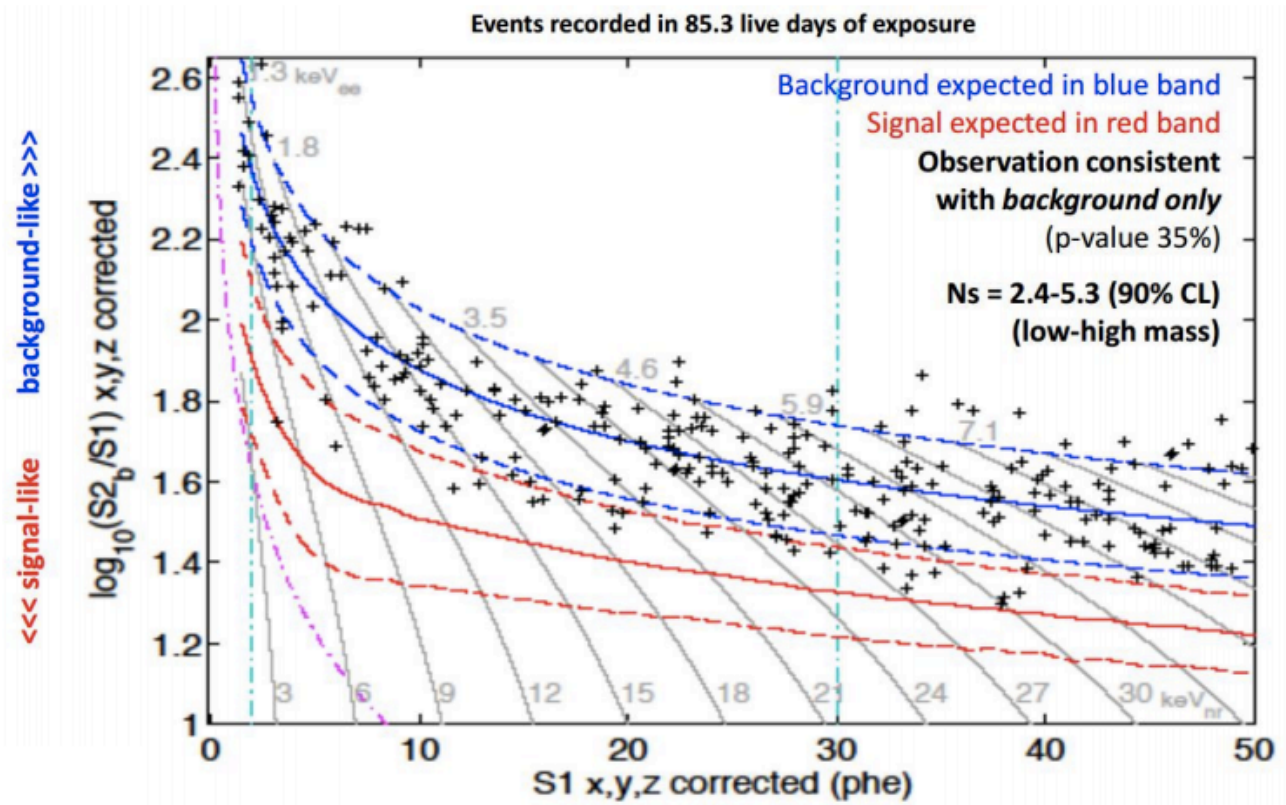

The LUX First WIMP-Search Result And Beyond...

- **To date, LUX has set the world's best limit on spin-independent WIMP-nucleon elastic scattering cross-section:**

  7.6×10^{-46} cm^2 for 33 GeV-WIMPs

- **Since the end of the first run:**
  - **New NR calibration using mono-energetic neutrons from DD source => improved sensitivity at low masses**
  - **Re-analysis with improved low energy threshold to be published this summer**
- **300-live-day run currently underway**
  - **Extending sensitivity by a factor of ~5**
  - **Discovery still possible!**

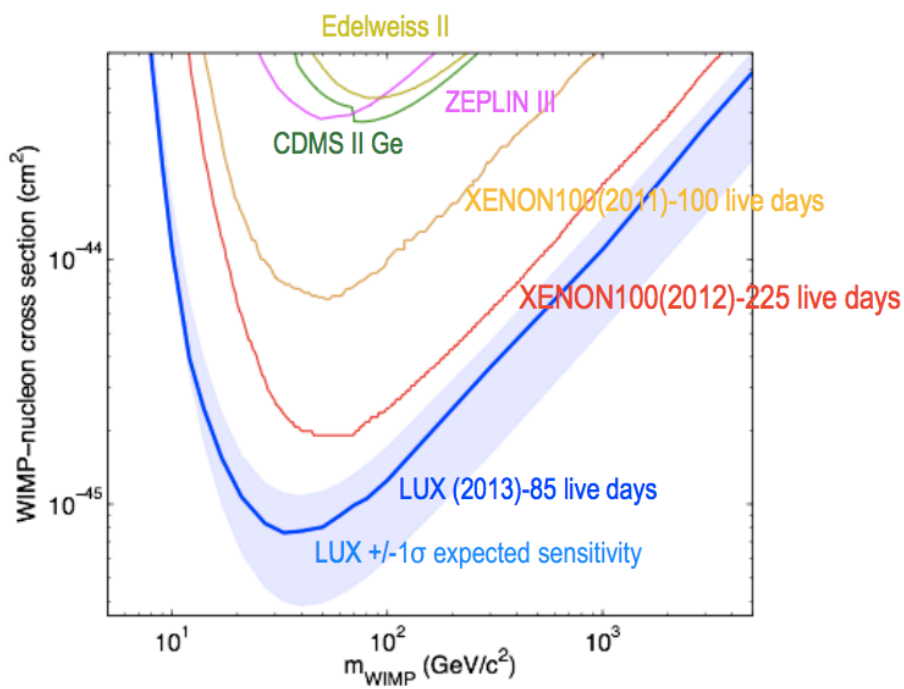

LUX 2013 result: PRL.112.091303 (arXiv:1310.8214)

Direct Detection Basics

- **In general, the formula for scattering rate of WIMPs off a target is:**

$$\frac{\mathrm{d}R}{\mathrm{d}|q^2|} = \left\langle \frac{\rho_0}{m_\chi m_A} \frac{\mathrm{d}\sigma}{\mathrm{d}|q^2|} \right\rangle$$

<…> denotes average over the WIMP velocity distribution

- **The differential cross-section for spin-independent WIMP-nucleon elastic scattering is:**

$$\frac{\mathrm{d}\sigma}{\mathrm{d}|q^2|} = \frac{1}{\pi v^2}|\mathcal{M}|^2 = \frac{\sigma_{0\chi A}}{4\mu_A^2 v^2} F^2(q) = \frac{\sigma_0}{4\mu_N^2 v^2} A^2 F^2(q)$$

In general

Assume non-vanishing in the limit of small q

For SI scattering

We can only factor the scattering matrix amplitude $|M|^2$ in this way if the interaction does not vanish for small momentum transfers *q*.

SI, SD interactions are the only interactions that do not vanish in the zero-momentum-transfer limit – this is why direct detection experiments like LUX typically only present SI and SD limits.

New WIMP-Nucleon Interactions

- SI+SD-only analyses assume that momentum transfers involved in WIMP-nucleus scatters are nonrelativistic.
- However:
  - The usual SI and SD interactions could be suppressed…
  - Momentum transfer is not necessarily small on a parton scale…

There are several momentum- and velocity-dependent interactions also allowed by basic symmetry considerations.

- Novel nuclear responses such as angular-momentum-dependent (LD) and angular-momentum/spin-dependent (LSD) responses are allowed.
- These LD and LSD responses can interfere with the SI and SD responses.

References: Fitzpatrick et al. arXiv:1203.3542, 1211.2818
Anand et al. arXiv: 1308.6288, 1405.6690
Cirelli et al. arXiv:1307.5955

Studying the New Interactions

GOAL 1: **Investigate the extent to which momentum/velocity-dependent interactions affect our signal in xenon.**

GOAL 2: **For a given target material (xenon), optimize analysis techniques to best probe these momentum/velocity-dependent interactions.**

GOAL 3: **(General) Check that the array of direct detection target materials currently in use do not leave any "blind spots" in WIMP parameter space.**

The Effective Field Theory Setup

- **WIMP-nucleon elastic scattering is analogous to a four-fermion contact interaction in standard weak interaction theory.**

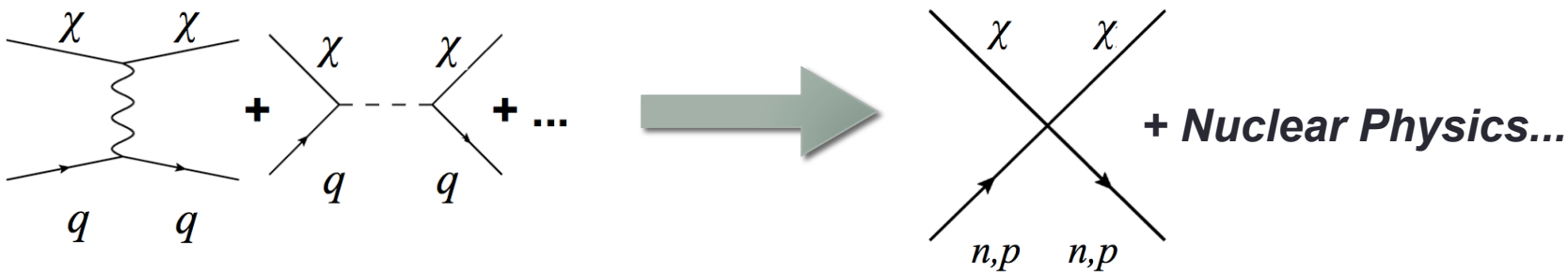

- **The general interaction Lagrangian:**

$$\mathcal{L}_{\rm int} = c\ \Psi_\chi^* \mathcal{O}_\chi \Psi_\chi\, \Psi_N^* \mathcal{O}_N \Psi_N = \sum_{i=1}^{\mathcal{N}} \left(c_i^{(n)} \mathcal{O}_i^{(n)} + c_i^{(p)} \mathcal{O}_i^{(p)} \right)$$

- **Restrict to operators O_i that are Galilean-invariant and Hermitian.**
- **Remaining O_i's are combinations of WIMP spin S_χ, nucleon spin S_N, incident velocity v^2, and momentum transfer q^2.**
- **Allow the O_i's to be at most quadratic in v (i.e. restrict to exchange of a spin-0 or spin-1 boson) and q (absorb higher powers of q into form factors).**

The Set of Allowed EFT Operators

SI Interaction

Cannot obtain at lowest order

SD Interaction

$$\mathcal{O}_1 = 1_\chi 1_N$$
$$\mathcal{O}_2 = (v^\perp)^2$$
$$\mathcal{O}_3 = i\vec{S}_N \cdot (\frac{\vec{q}}{m_N} \times \vec{v}^\perp)$$
$$\mathcal{O}_4 = \vec{S}_\chi \cdot \vec{S}_N$$
$$\mathcal{O}_5 = i\vec{S}_\chi \cdot (\frac{\vec{q}}{m_N} \times \vec{v}^\perp)$$
$$\mathcal{O}_6 = (\vec{S}_\chi \cdot \frac{\vec{q}}{m_N})(\vec{S}_N \cdot \frac{\vec{q}}{m_N})$$
$$\mathcal{O}_7 = \vec{S}_N \cdot \vec{v}^\perp$$
$$\mathcal{O}_8 = \vec{S}_\chi \cdot \vec{v}^\perp$$
$$\mathcal{O}_9 = i\vec{S}_\chi \cdot (\vec{S}_N \times \frac{\vec{q}}{m_N})$$
$$\mathcal{O}_{10} = i\vec{S}_N \cdot \frac{\vec{q}}{m_N}$$
$$\mathcal{O}_{11} = i\vec{S}_\chi \cdot \frac{\vec{q}}{m_N}$$

- **Each nuclear form factor F_{ij} associated with the EFT operators can be written as a linear combination of five macroscopic nuclear responses that depend only on the nuclear physics: (arXiv:1203.3542)**

M	Σ'	Σ''	Δ	Φ''
SI response	SD response (longitudinal component)	SD response (transverse component)	LD (angular-momentum-dependent) response	LSD (spin-orbit) response

Converting Between the EFT Operators and the Macroscopic Nuclear Responses

	M (SI)	Σ'' (SD long.)	Σ' (SD trans.)	Δ (LD)	Φ'' (LSD)
O_1	q-indep.				
O_3			$\sim q^4, q^2v^2$		$\sim q^4$
O_4		q-indep.	q-indep.		
O_5	$\sim q^4, q^2v^2$			$\sim q^4$	
O_6		$\sim q^4$			
O_7			$\sim q^2, v^2$		
O_8	$\sim q^2, v^2$			$\sim q^2$	
O_9			$\sim q^2$		
O_{10}		$\sim q^2$			
O_{11}	$\sim q^2$				

Comparing Target Materials

- **Estimate the number of predicted events as:**

$$\frac{dN}{dE_R} \sim 5000\text{keV}^{-1}\left(\frac{\text{exposure}}{\text{kg}\cdot\text{day}}\right)\left(\frac{100\text{GeV}}{m_\chi}\right)^3 \mathcal{L}_{\text{int}}^2$$

- **Comparing the interaction terms for different targets:**

	S_n^2	S_p^2	L_n^2	L_p^2	$(S_n \cdot L_n)^2$	$(S_p \cdot L_p)^2$
F	$8 \cdot 10^{-5}$	0.2	0.04	0.05	0.6	0.1
Na	0.0004	0.06	0.1	0.8	5.5	3.3
Ge	0.02	$5 \cdot 10^{-6}$	1.1	0.003	35	100
I	0.004	0.07	0.4	2.	100	500
Xe	0.02	$2 \cdot 10^{-5}$	0.4	0.04	500	300

(arXiv:1211.2818)

- **Xenon is sensitive to not only SD WIMP-neutron interactions, but also to the new LD (Δ) and LSD (Φ'') interactions for both nucleons.**

SI and LD WIMP-n Recoil Spectra

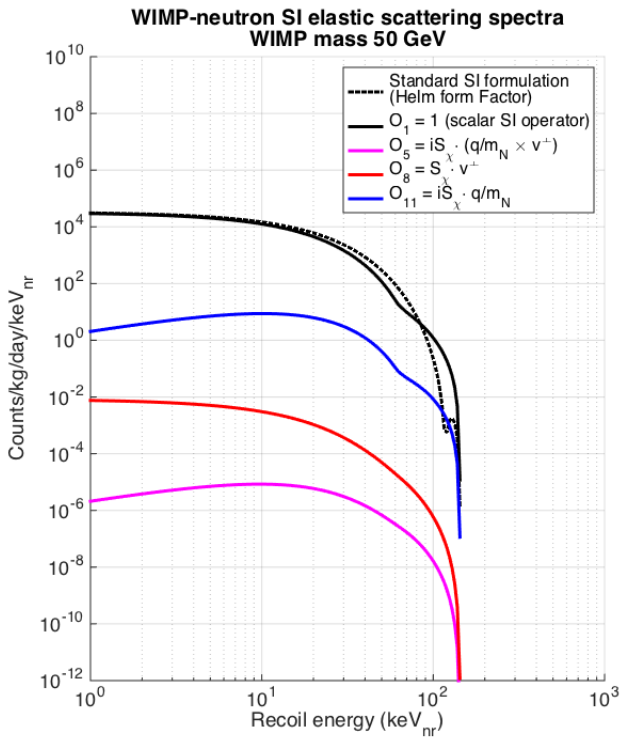

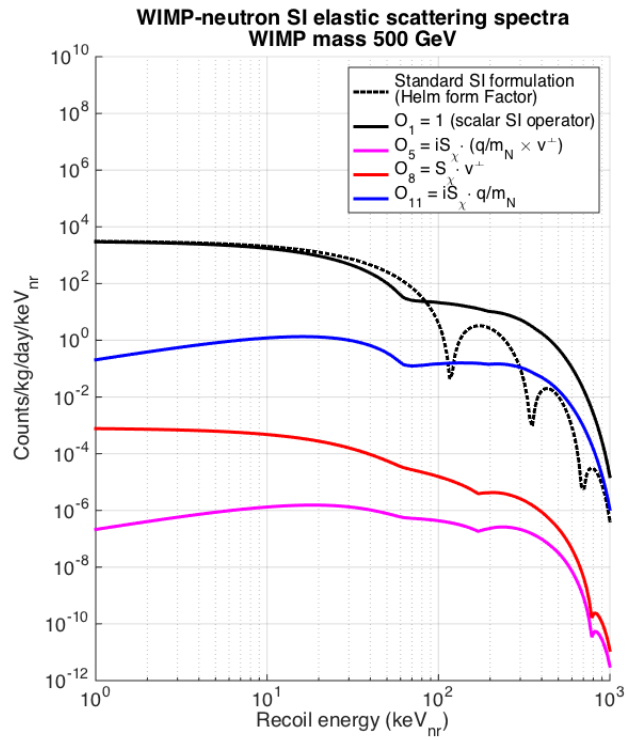

- O_1 (the usual SI interaction) and O_{11} both produce an SI response, but the spectra have different slopes due to different *q*-dependence.
- O_5 and O_8 each produce both an LD and an SI response, again with different *q*-dependence.
- For m_{WIMP} large, the EFT spectra stay relatively flat out to ~few hundred keV.

SD and LSD WIMP-n Recoil Spectra

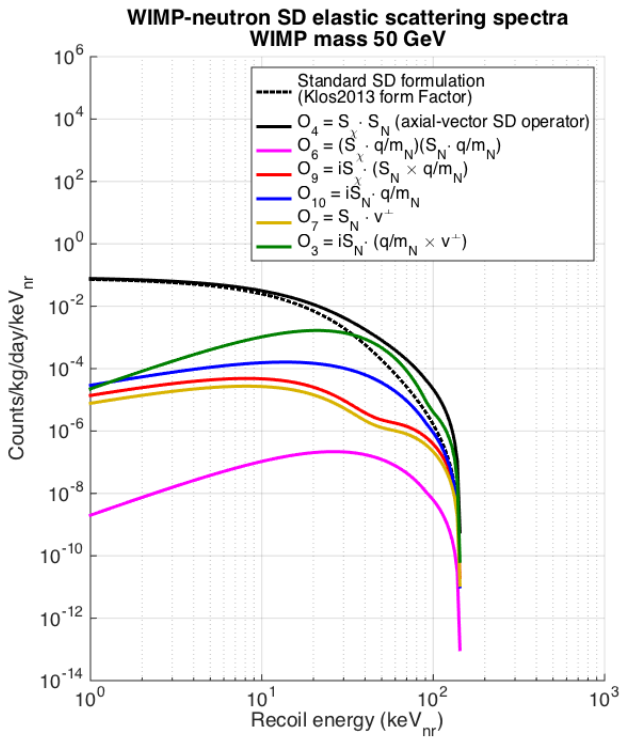

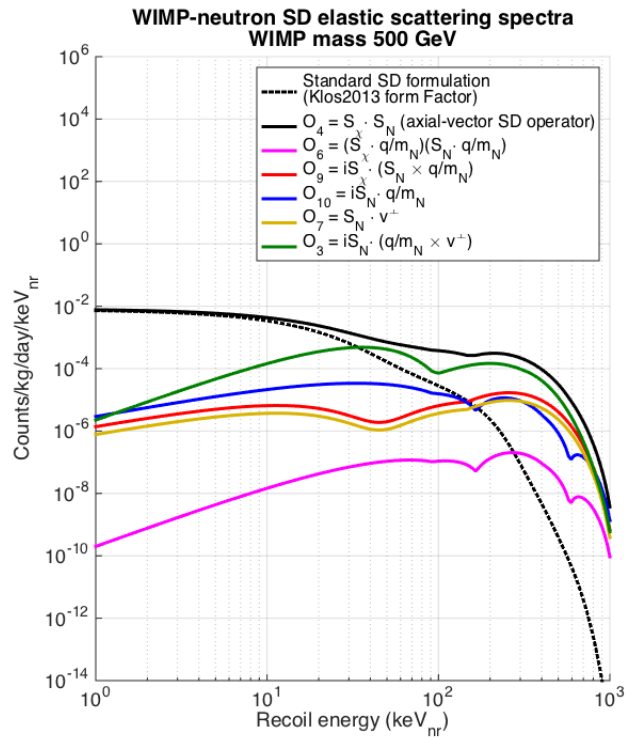

- **The two types of SD response (transverse and longitudinal to the momentum transfer *q*) exhibit distinctly different behaviors.**
- **Again the slope of the spectrum depends on the *q*-dependence of the operator.**
- **O_3 (green) is the only LSD operator. Its spectrum increases sharply to around 50 keV and does not begin to decrease until ~300 keV for heavy WIMPs.**

Optimizing the WIMP-Search Window

Table: The minimum upper bound on the WIMP-search window in keVnr for the WIMP-search region to contain 50% or 90% of the integrated spectrum

	Operator	50-GeV WIMP		500-GeV WIMP	
		50%	90%	50%	90%
SI	Standard SI	10.8	27.3	16.6	44.7
	O_1	9.9	24.6	14.7	42.4
	O_{11}	16.4	34.4	39.8	281
SI + LD	O_5	15.3	32.8	36.5	243
	O_8	9.3	23.0	14.9	43.4
SD	Standard SD	8.6	21.6	11.9	37.5
	O_4	10.0	27.6	48.8	310
	O_6	33.6	64.1	268	434
	O_9	14.4	38.6	277	463
	O_{10}	22.2	49.0	113	342
	O_7	14.4	38.6	277	463
SD + LSD	O_3	26.3	49.2	142	346

For many of the new momentum-dependent operators, we require a search window of up to several hundred keVnr to capture most of the signal.

Constraints on Representative Operators

- **On the next slide I show projected cut-and-count limits for the LUX 2013 run and for LZ (the 7-ton successor to LUX)**
- **Relevant parameters:**

	LUX 2013	LZ (Projected)
Fiducial Mass	118 kg	5600 kg
Livetime	85.3 d	1000 d
Standard energy window	3-25 keVnr	6-30 keVnr
Background events expected	0.6	1.9
Events observed	0	-
Standard Maxwellian dark matter velocity distribution, etc…		

- **For "optimized" energy window (different upper threshold for each operator depending on peak of spectrum) assume background scales linearly with size of window (very conservative).**
- **For LZ assume num. events observed = num. background events expected.**

Constraints on Representative Operators

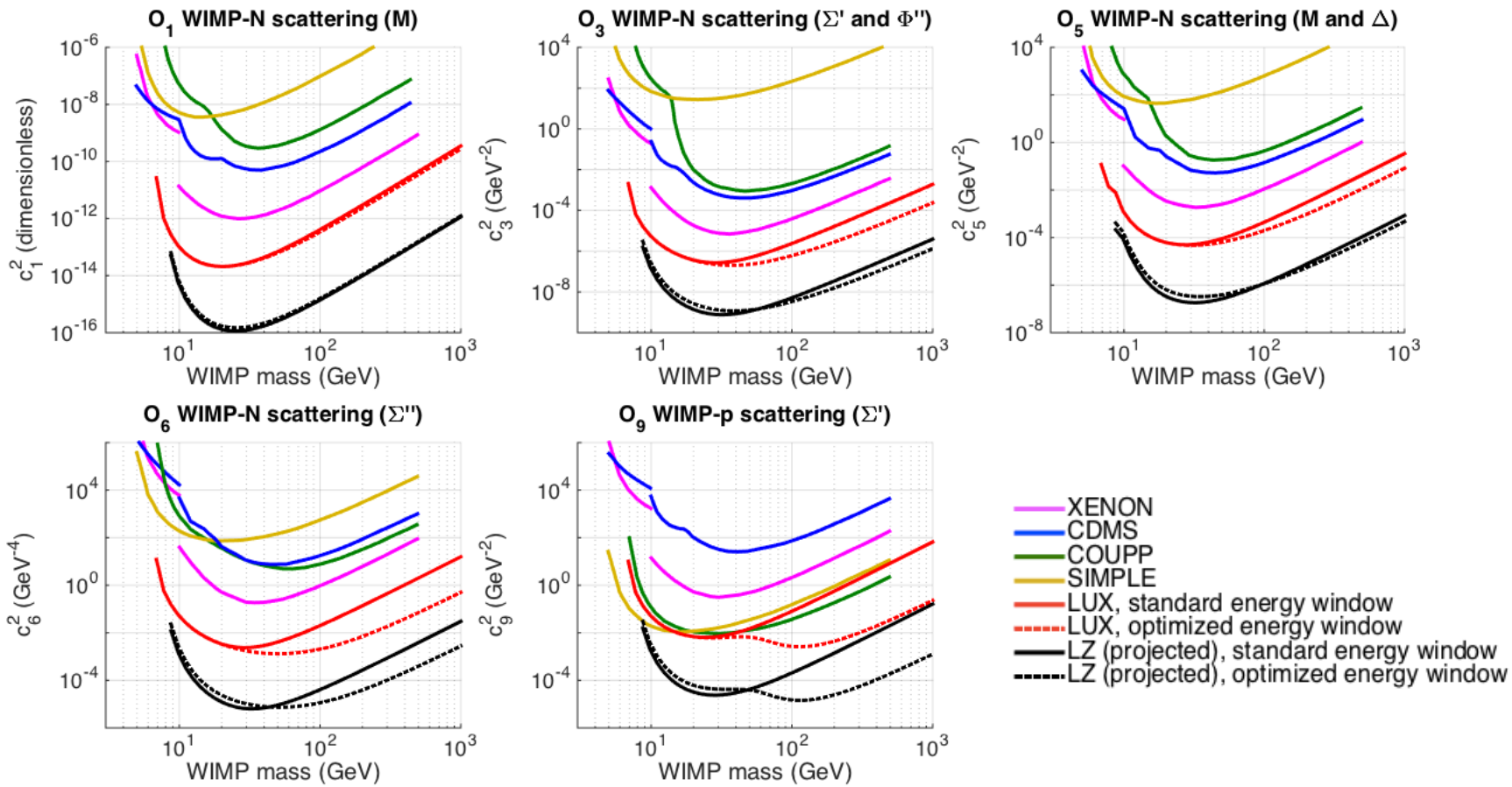

Effects of Changing the Energy Window

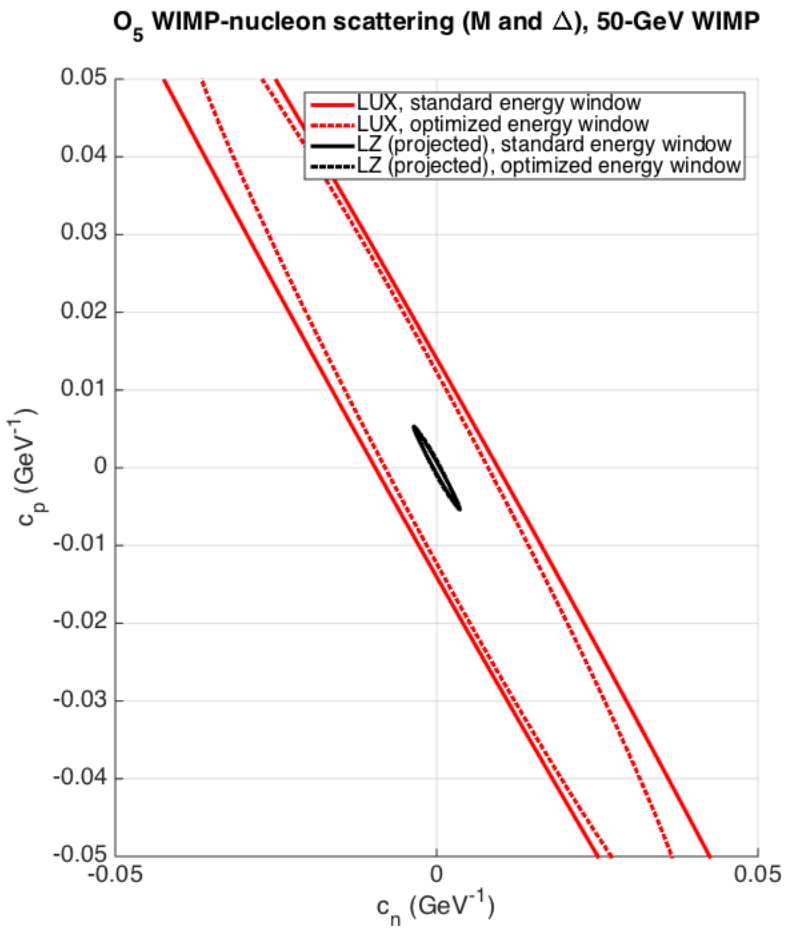

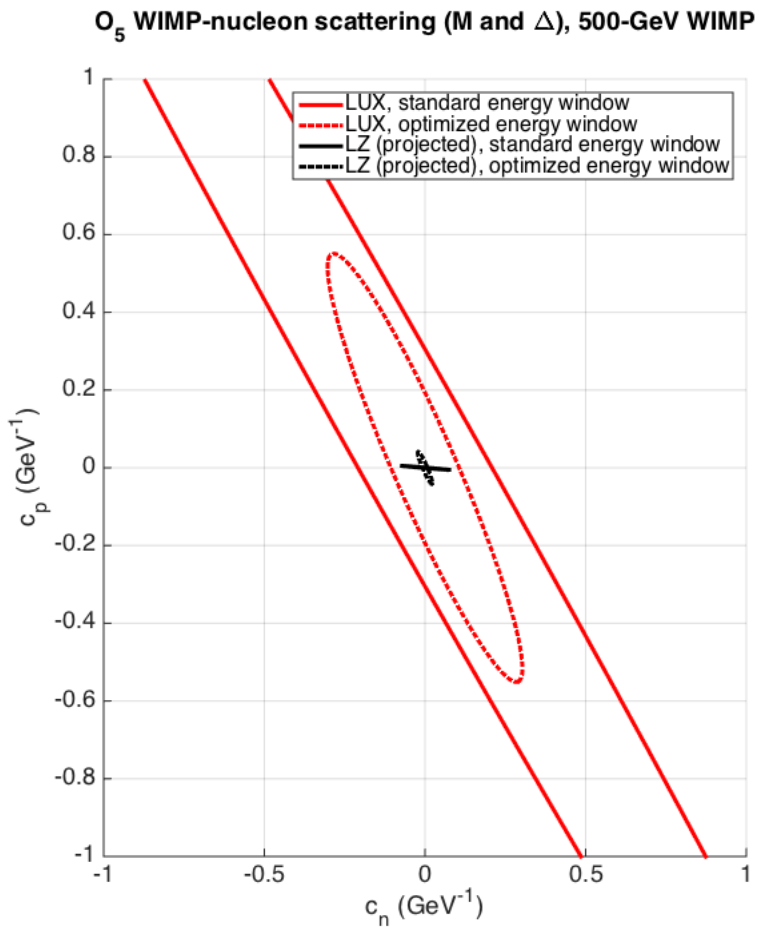

Summary and Next Steps

- Direct detection experiments traditionally only present limits on interactions that vanish in the zero-momentum-transfer limit (SI and SD), but there are 8 other operators that can produce momentum-dependent SI and SD responses as well as new nuclear responses (LD, LSD)
- Signal models have been generated and both cut-and-count and PLR limits (not shown) have been produced for the LUX 2013 run, and cut-and-count limit projections have been produced for LZ
- Extending the WIMP search window allows us to optimize signal-to-background based on where the each operator's spectrum peaks
- At higher recoil energies pulse-shape cuts and other discrimination techniques can be used to help with signal-to-noise ratio (ongoing investigation)
- Compare to SuperCDMS paper (ArXiv 1503.03379v1)

Thank you!

Brown

Richard Gaitskell	PI, Professor
Simon Fiorucci	Research Associate
Samuel Chung Chan	Graduate Student
Dongqing Huang	Graduate Student
Casey Rhyne	Graduate Student
Will Taylor	Graduate Student
James Verbus	Graduate Student

Imperial College London

Henrique Araujo	PI, Reader
Tim Sumner	Professor
Alastair Currie	Postdoc
Adam Bailey	Graduate Student
Khadeeja Yazdani	Graduate Student

Lawrence Berkeley + UC Berkeley

Bob Jacobsen	PI, Professor
Murdock Gilchriese	Senior Scientist
Kevin Lesko	Senior Scientist
Peter Sorensen	Scientist
Victor Gehman	Scientist
Attila Dobi	Postdoc
Daniel Hogan	Graduate Student
Mia Ihm	Graduate Student
Kate Kamdin	Graduate Student
Kelsey Oliver-Mallory	Graduate Student

Lawrence Livermore

Adam Bernstein	PI, Leader of Adv. Detectors Grp.
Kareem Kazkaz	Staff Physicist
[illegible]enardo	Graduate Student

LIP Coimbra

Isabel Lopes	PI, Professor
Jose Pinto da Cunha	Assistant Professor
Vladimir Solovov	Senior Researcher
Francisco Neves	Auxiliary Researcher
Alexander Lindote	Postdoc
Claudio Silva	Postdoc

SLAC Nation Accelerator Laboratory

Dan Akerib	PI, Professor
Thomas Shutt	PI, Professor
Kim Palladino	Project Scientist
Tomasz Biesiadzinski	Research Associate
Christina Ignarra	Research Associate
Wing To	Research Associate
Rosie Bramante	Graduate Student
Wei Ji	Graduate Student
T.J. Whitis	Graduate Student

SD School of Mines

Xinhua Bai	PI, Professor
Doug Tiedt	Graduate Student

SDSTA

David Taylor	Project Engineer
Mark Hanhardt	Support Scientist

Texas A&M

James White †	PI, Professor
Robert Webb	PI, Professor
Rachel Mannino	Graduate Student
Paul Terman	Graduate Student

University at Albany, SUNY

Matthew Szydagis	PI, Professor
Jeremy Mock	Postdoc
Steven Young	Graduate Student

UC Davis

Mani Tripathi	PI, Professor
Britt Hollbrook	Senior Engineer
John Thmpson	Development Engineer
Dave Herner	Senior Machinist
Ray Gerhard	Electronics Engineer
Aaron Manalaysay	Postdoc
Scott Stephenson	Postdoc
Jacob Cutter	Graduate Student
James Morad	Graduate Student
Sergey Uvarov	Graduate Student

UC Santa Barbara

Harry Nelson	PI, Professor
Mike Witherell	Professor
Susanne Kyre	Engineer
Dean White	Engineer
Carmen Carmona	Postdoc
Scott Haselschwardt	Graduate Student
Curt Nehrkorn	Graduate Student
Melih Solmaz	Graduate Student

University College London

Chamkaur Ghag	PI, Lecturer
Sally Shaw	Graduate Student

University of Edinburgh

Alex Murphy	PI, Reader
Paolo Beltrame	Research Fellow
James Dobson	Postdoc
Tom Davison	Graduate Student
Maria Francesca Marzioni	Graduate Student

University of Maryland

Carter Hall	PI, Professor
Jon Balajthy	Graduate Student
Richard Knoche	Graduate Student

University of Rochester

Frank Wolfs	PI, Professor
Wojtek Skutski	Senior Scientist
Eryk Druszkiewicz	Graduate Student
Dev Ashish Khaitan	Graduate Student
Mongkol Moongweluwan	Graduate Student

University of South Dakota

Dongming Mei	PI, Professor
Chao Zhang	Postdoc
Angela Chiller	Graduate Student
Chris Chiller	Graduate Student

Yale

Daniel McKinsey	PI, Professor
Ethan Bernard	Research Scientist
Markus Horn	Research Scientist
Blair Edwards	Postdoc
Scott Hertel	Postdoc
Kevin O'Sullivan	Postdoc
Elizabeth Boulton	Graduate Student
Nicole Larsen	Graduate Student
Evan Pease	Graduate Student
Brian Tennyson	Graduate Student
Lucie Tvrznikova	Graduate Student